Entanglement from the Diósi–Penrose Model: An Exact Criterion, and Why It Stays Small at Any Distance

Marc Sperzel*

Independent Researcher

November 11, 2026

Abstract

Trillo and Navascués showed that the Diósi–Penrose model, in the Tilloy–Diósi form with the same smearing length σ in force and noise, entangles two masses in superposition when they are closer than about $2.2\,\sigma$, and asked whether gravitationally induced entanglement can be observed beyond that distance. We answer for two rigid bodies whose branches are position eigenstates on finite sets, without kinetic term, for noise strength C. A product state becomes entangled if and only if the largest canonical correlation between neutral charge patterns on the two branch sets, in the Coulomb energy of the smeared bodies, exceeds $C/\sqrt{1+C^2}$. Below this threshold the evolution is a separable operation at all times, with an explicit decomposition into independent pairs, to each of which a lemma of Wang, Pedernales and Plenio applies. The published critical distances are two-branch cases of the criterion: for parallel two-branch superpositions the supremum is $2.21\,\sigma$ at $C = 1$, and a straddling geometry reaches $2.74\,\sigma$. With many branches there is no critical distance. What limits the effect is the model's own decoherence. The entangling rate is at most the fraction $(\sqrt{\pi}/C)(\sqrt{1+C^2} - C)\,\sigma_{\mathrm{eff}}/d$ of the single-body dephasing rate, and at most $0.12\,\sigma_{\mathrm{eff}}/d$ for slab-separated supports at $\sigma \ll d$ and $C = 1$. The entanglement is transient: its negativity stays below $0.19\,\sigma_{\mathrm{eff}}/d$ for branches more than a few σ apart, and is about $10^{-2}\,\sigma_{\mathrm{eff}}/d$ by a leading-order law, against 0.4 for unitary Newtonian gravity on the same states. Entanglement of the size unitary gravity predicts still excludes the model; the inference from any detected entanglement beyond a fixed multiple of σ does not hold.

1 Introduction

Two masses, each in a superposition of positions, become entangled through their gravitational interaction if gravity is a quantum channel; the detection of that entanglement has been proposed as a witness of the quantum nature of gravity [1, 2]. The witness needs a classical benchmark. The Diósi–Penrose model [3, 4, 5], in the form of Tilloy and Diósi [6, 7], is one: a classical Newtonian field sourced by continuously monitored, σ-smeared mass densities, with a decoherence that the positivity of the dynamics forces [8]. Trillo and Navascués showed that this model does entangle two masses, in the same geometries in which the quantum prediction is made [9]. For two branches per mass they found critical distances, $0.850872\,\sigma$ for collinear superpositions of

*ORCID: 0009-0000-6252-3155. Email: me@marcsperzel.com

vanishing size and $2.21093\,\sigma$ for transversal superpositions of diverging size, and asked: "Is there a way to observe GIE beyond d_c?" Later work quotes $d_c \approx 0.85\,\sigma$ as the separation below which the model entangles [10, 11]; that statement is correct for small packets with two branches, and it is the general reading of it that this paper corrects. Wang, Pedernales and Plenio, in a study of local error correction, gave a separability lemma for one pair of coupled operators, found the Diósi–Penrose dynamics of their two-level codes separable outside a small region of d/σ, and left the exact classification as "beyond our scope" [12].

This paper gives that classification for position branches and draws the consequences. The result has two parts.

The criterion (Theorem 2.2). With no kinetic term, two rigid bodies in a product state on finite sets of position branches become entangled if and only if

$$\rho_{\max}(S_A, S_B) \;>\; \frac{C}{\sqrt{1+C^2}}, \tag{1}$$

where $\rho_{\max}$ is the largest canonical correlation [13], in the Coulomb energy of the smeared bodies, between neutral charge patterns on the two branch sets, and $C \geq 1$ is the noise strength ($C = 1$ in [9]). Below the threshold the evolution is a separable operation for all time. The criterion depends on the branch sets, σ, the body shape and C; not on the masses, the amplitudes or the time.

The size (Sections 4 and 5). With many branches the threshold is exceeded at every separation, so there is no critical distance. But the rate at which entanglement is produced is a small fixed fraction of the rate at which each body dephases under the same dynamics,

$$\frac{\Gamma_{\text{ent}}}{\Gamma_{\text{sat}}} \;=\; \frac{\sqrt{\pi}\,\kappa}{C}\,\frac{\sigma_{\text{eff}}}{d} \;\leq\; 0.12\,\frac{\sigma_{\text{eff}}}{d} \qquad (C = 1,\ \text{slab-separated supports},\ \sigma \ll d), \tag{2}$$

with κ a dimensionless rate constant, $\Gamma_{\text{sat}} = C\,Gm^2/(\sqrt{\pi}\,\hbar\,\sigma_{\text{eff}})$ the saturated Diósi–Penrose dephasing rate, and $\sigma_{\text{eff}} = \sigma$ for point masses. The negativity peaks at about $\Gamma_{\text{ent}}/(2e\Gamma_{\text{sat}})$, half a dephasing time after preparation. Section 5 applies both parts to the design of Bose *et al.* [1]; Section 6 lists what is not controlled.

2 The model and the criterion

2.1 The master equation in the position basis

The Tilloy–Diósi dynamics with smeared force and noise, in the notation of [9] with a noise strength C, is

$$\dot\rho = -\frac{i}{\hbar}[H,\rho] + \frac{G}{2\hbar}\iint \frac{d^3r\,d^3s}{|\mathbf{r}-\mathbf{s}|}\Big(- C\,[\mu_\sigma(\mathbf{r}),[\mu_\sigma(\mathbf{s}),\rho]] + i\,[\mu_\sigma(\mathbf{r})\mu_\sigma(\mathbf{s}),\rho]\Big), \tag{3}$$

with μ_σ the mass density smeared by a normalised Gaussian of standard deviation σ. The second term is the Newtonian interaction of the smeared densities, the first the monitoring noise. In measurement-and-feedback realisations $C \geq 1$, and $C = 1$ is the least-decoherence point [6, 7]; $C = 1$ is the case of [9].

Two rigid bodies A, B with masses m_A, m_B carry their centres as quantum degrees of freedom. Let g_a be the σ-smeared unit-mass density of body A centred at a, and g_b that of B.

On charge densities use the Coulomb form $\langle u, v\rangle = \iint u(x)v(y)/|x-y|$ and put

$$f_A(a,a') = \langle g_a, g_{a'}\rangle, \qquad f_B(b,b') = \langle g_b, g_{b'}\rangle, \qquad F(a,b) = \langle g_a, g_b\rangle. \tag{4}$$

For point masses all three equal $f(r) = \operatorname{erf}(r/2\sigma)/r$, with $f(0) = f_0 = 1/(\sqrt{\pi}\,\sigma)$. With $H = 0$, Eq. (3) acts on position matrix elements multiplicatively,

$$\rho_t(ab, a'b') = \rho_0(ab, a'b')\, \exp\Big[\frac{Gt}{\hbar}\,\Lambda(ab, a'b')\Big], \tag{5}$$

$$\Lambda = i\, m_A m_B\big[F(a,b) - F(a',b')\big] - \frac{C}{2}\,\big\|m_A(g_a - g_{a'}) + m_B(g_b - g_{b'})\big\|^2. \tag{6}$$

The norm is the Coulomb norm. Expanded, the real part is $-C\,[m_A^2 D_A + m_B^2 D_B + m_A m_B\,\delta]$ with $D_A = f_A(a,a) - f_A(a,a')$ and $\delta = F(a,b) + F(a',b') - F(a,b') - F(a',b)$. The local terms D_A, D_B are the Diósi–Penrose dephasing of each body; δ is the correlated part of the noise.

2.2 The criterion

A state is a *branch state* on finite sets S_A, S_B of centre positions if it is supported on $S_A \times S_B$; for a product state $\psi_A \otimes \psi_B$ write $p_a = |\psi_A(a)|^2$, $r_b = |\psi_B(b)|^2$. The branches are position eigenstates (Section 6 discusses wavepackets).

Definition 2.1. Let $V_A = \operatorname{span}\{g_a - g_{a'} : a, a' \in S_A\}$ and V_B likewise: the neutral charge patterns on the branch sets. Their largest Coulomb canonical correlation is

$$\rho_{\max}(S_A, S_B) = \sup\Big\{\frac{|\langle u, v\rangle|}{\|u\|\,\|v\|} :\ u \in V_A,\ v \in V_B\Big\}, \qquad s_*(C) = \frac{C}{\sqrt{1+C^2}}. \tag{7}$$

$\rho_{\max}$ is the top singular value of $f_A^{-1/2} F f_B^{-1/2}$ restricted to zero-sum vectors; it does not depend on the masses. $s_*(1) = 1/\sqrt{2} = 0.7071$.

Theorem 2.2 (Entanglement criterion)**.** *Let $H = 0$ and $C > 0$, and let S_A, S_B be finite sets of distinct branches.*

(a) If $\rho_{\max} > s_*$, every pure product state with all amplitudes non-zero has a partial transpose with a negative eigenvalue for all sufficiently small $t > 0$. That eigenvalue leaves zero at the rate

$$\dot\lambda = \frac{G}{\hbar}\min_{q_1, q_2} \frac{C m_A^2\langle q_1, q_1\rangle + C m_B^2\langle q_2, q_2\rangle - 2 m_A m_B\,\mathrm{Re}\big[(C+i)\langle q_1, q_2\rangle\big]}{\sum_a |q_1(a)|^2/p_a + \sum_b |q_2(b)|^2/r_b}, \tag{8}$$

the minimum over neutral complex patterns q_1 on S_A and q_2 on S_B, with $\langle q_1, q_2\rangle = \sum_{ab} \bar q_1(a) q_2(b) F(a,b)$ and $\langle q_1, q_1\rangle = \sum \bar q_1(a) q_1(a') f_A(a,a')$.

(b) If $\rho_{\max} \le s_*$, the evolution restricted to $S_A \times S_B$ is a separable operation for every $t \ge 0$: a mixture of products of local completely positive maps. Every separable initial state stays separable, also when local channels acting within the branch spaces are interleaved.

(c) Hence the model entangles some product state on $S_A \times S_B$ at some time if and only if it entangles every full-support pure product state at first order, if and only if $\rho_{\max} > s_*$.

Proof sketch. (a) Partial transposition exchanges $a \leftrightarrow a'$, and $\rho_0^{T_1}$ is a rank-one projector. For a vector χ orthogonal to it put $c = \tilde{\Psi}^* \chi$ entrywise, $\tilde{\Psi} = \bar{\psi}_A \otimes \psi_B$, so that $\sum c = 0$. At first order in t every term of Λ that depends on (a, b) alone or on (a', b') alone drops out of $\langle \chi | \rho_t^{T_1} | \chi \rangle$, and with the marginals $q_1(a) = \sum_b c(ab)$, $q_2(b) = \sum_a c(ab)$ what remains is the numerator of Eq. (8). Every pair of neutral patterns arises, through $c = q_1 \otimes r + p \otimes q_2$, which also minimises $\|\chi\|^2$ at given marginals and gives the denominator. Optimising the phase and the scale of q_2, the numerator is negative for some pair if and only if $|\langle q_1, q_2 \rangle|^2 > s_*^2 \langle q_1, q_1 \rangle \langle q_2, q_2 \rangle$, that is, if and only if $\rho_{\max} > s_*$; the state is then entangled by the Peres criterion [14].

(b) Choose bases of V_A and V_B that diagonalise the cross form (a singular value decomposition with singular values $s_i \le \rho_{\max}$) and let $x_i(a)$, $y_i(b)$ be the coordinates of the branches in them. Since one kernel F enters both the force and the correlated noise, and the local dephasing is the Gram form used for the whitening,

$$\Lambda = \sum_i \Lambda_i + (\text{local phases}), \qquad \Lambda_i = i s_i (x_i y_i - x_i' y_i') - \tfrac{C}{2}(x_i - x_i')^2 - \tfrac{C}{2}(y_i - y_i')^2 - C s_i (x_i - x_i')(y_i - y_i'), \tag{9}$$

with no terms coupling different i (masses absorbed into g). Each Λ_i is reproduced by random local phase-and-amplitude multipliers $e^{x_i(\eta_i + i\zeta_i)}$, $e^{y_i(\eta_i' + i\zeta_i')}$ with Gaussian latent variables, up to a local Schur multiplier with exponent $t\,(C - s_i\sqrt{1+C^2})\, x_i x_i'$. When $s_i\sqrt{1+C^2} \le C$ for every i that multiplier is positive semidefinite, hence completely positive, and ρ_t is an average of products of local completely positive maps applied to ρ_0. Appendix A gives the covariance and the bookkeeping. (c) follows from (a) and (b). □

Remark 2.1 (Generality). The proof uses only that one real cross kernel enters both the Hamiltonian and the correlated noise and that the local dephasing is the Gram form. Theorem 2.2 therefore holds for any real cross kernel $\bar{F}$ with $\rho_{\max}$ replaced by the top singular value of $f_A^{-1/2} \bar{F} f_B^{-1/2}$ on neutral vectors, provided that value is at most one (otherwise the noise is not positive). Theorem 4.2 below uses this for $\bar{F} = \theta F$.

Remark 2.2 (Relation to Wang, Pedernales and Plenio). Each Λ_i in Eq. (9) is the generator of Lemma 3 of [12] with $O_A = \sum_a x_i(a) |a\rangle\langle a|$, $O_B = \sum_b y_i(b) |b\rangle\langle b|$, coupling $\lambda = -s_i$, local rates $\Gamma_A = \Gamma_B = C$ and cross rate $\Gamma_{AB} = -C s_i$ (in units $Gm^2/\hbar\sigma$). Their lemma makes $e^{t\Lambda_i}$ separable when $\lambda^2 + \Gamma_{AB}^2 \le \Gamma_A \Gamma_B$, which is $s_i\sqrt{1+C^2} \le C$. Part (b) therefore also follows from their lemma applied pair by pair, for one reason: the canonical decomposition leaves no cross terms between pairs, so $e^{t\Lambda}$ is a product of separable channels up to a local unitary. That the Λ_i commute is automatic for position-diagonal generators and is not the reason; for several coupled operators a pairwise condition does not in general give a joint one (cf. their Theorem 1). With an unsmeared force, force and noise have different kernels, no single decomposition diagonalises both, and the pairwise argument fails for three or more branches. Necessity for any number of branches is part (a).

Two features of the threshold are worth stating. The noise helps: dephasing alone would give the threshold 1, never reached; the Hamiltonian supplies the i and the correlated noise the C in $C + i$, and $|C + i| = \sqrt{1 + C^2}$ lowers the threshold to $s_* < 1$. And mode by mode the generator is never positive: for one Fourier mode the two-by-two form has determinant $C^2 - (1 + C^2) = -1$, so separability comes only from the two bodies occupying different regions.

Remark 2.3 (The idealisation). Potentials of smeared charges are real-analytic, so the smeared

point charges of any open set span the whole Coulomb space: $\rho_{\max} = 1$ for any two supports with interior. Every pair of square-integrable wavefunctions is therefore entangled at once, at every separation (Theorem A.1 in Appendix A gives the entangling direction in L^2). The "if and only if" of Theorem 2.2 is a statement about position-eigenstate branches, the idealisation also used in [9, 12]. The physical content lies in the rate and the size of the entanglement, Section 4.

3 Two-branch states, and why many branches have no critical distance

3.1 The published distances as special cases

For $S_A = \{a_1, a_2\}$, $S_B = \{b_1, b_2\}$ each V is one-dimensional and Eq. (7) is

$$s = \frac{|f(a_1b_1) + f(a_2b_2) - f(a_1b_2) - f(a_2b_1)|}{2\sqrt{D(L_A)D(L_B)}}, \qquad D(L) = f_0 - f(L), \tag{10}$$

with $L_A = |a_1 - a_2|$, $L_B = |b_1 - b_2|$ and $f(xy) = f(|x - y|)$ (point masses). Four limiting families have closed forms (Table 1, Fig. 1); each family increases monotonically towards its limit, which is not attained. With $\kappa_0 = -f''(0) = 1/(6\sqrt{\pi}\,\sigma^3)$: superpositions of length $L \to 0$ along the line joining the bodies give $|f''(d)|/\kappa_0$; transversal superpositions give $|f'(d)/d|/\kappa_0$ for $L \to 0$ and $f(d)/f_0 = \sqrt{\pi}\,\sigma\,\mathrm{erf}(d/2\sigma)/d$ for $L \to \infty$; and a vanishing superposition of A midway between two branches of B, each at distance d ("straddle"), gives $\sqrt{2}\,|f'(d)|/\sqrt{\kappa_0(f_0 - f(2d))}$. Setting each equal to s_* reproduces the two distances of [9] and adds two. The straddle limit exceeds the transversal one for $d < 3.699\,\sigma$, that is for every $C > 0.5396$.

Table 1. *Critical distances (in units of σ) of the limiting two-branch families, from limit $= s_*(C)$. d is the closest approach between branches of different bodies.*

family	limit of s	$C = 1$	$C = 1.25$	$C = 2$	$C = 5$
collinear, $L \to 0$ [9]	$\lvert f''(d)\rvert/\kappa_0$	0.850872			
transversal, $L \to 0$	$\lvert f'(d)/d\rvert/\kappa_0$	1.547134			
transversal, $L \to \infty$ [9]	$f(d)/f_0$	2.210928	1.8203	1.1845	0.4870
straddle	$\sqrt{2}\lvert f'(d)\rvert/\sqrt{\kappa_0(f_0 - f(2d))}$	2.738073	2.4425	1.9106	1.1832

Most designs give both masses the same superposition, translated; the design of [1] is one. For that class the transversal limit is the supremum.

Theorem 3.1 (Parallel superpositions)**.** *Let $S_A = \{a, a + w\}$ and $S_B = \{a + r, a + r + w\}$ for arbitrary vectors w, r, and let d be the closest approach. Then*

$$s \le \max\left(f(d)/f_0,\ c_*\right), \qquad c_* = \Lambda_+ L_{1/2}^2/f_0 = 0.634687, \tag{11}$$

where $\Lambda_+ = \max f'' = 0.311326\,\kappa_0$ (at $r = 3.2273\,\sigma$) and $f(L_{1/2}) = f_0/2$, $L_{1/2} = 3.497418\,\sigma$. For every $C \ge 0.8213$, in particular every $C \ge 1$, no parallel two-branch state with closest approach $d \ge d_*(C)$ is entangled, where $f(d_*)/f_0 = s_*(C)$ ($d_* = 2.210928\,\sigma$ at $C = 1$); for every $d < d_*(C)$ some are.

The proof (Appendix B) uses that $h(x) = f(\sqrt{x})$ is a mixture of decaying exponentials, hence

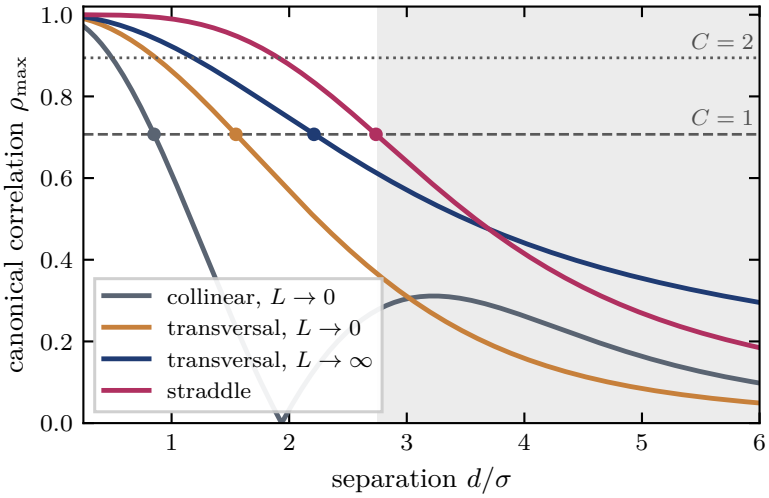


Figure 1. *Canonical correlation of the four limiting two-branch families against the separation, with the thresholds $s_*(1)$ and $s_*(2)$; dots mark the critical distances at $C = 1$. In the shaded region ($d \geq 2.75\,\sigma$ at slab separation) no two-branch state of any geometry is entangled at $C \geq 1$ (Proposition 3.2).*

convex and log-convex. For arbitrary two-branch geometries we have only computer-assisted ceilings.

Proposition 3.2 (Two-branch ceilings)**.** *For every $C \geq 1$ no two-branch state is entangled by the model at slab separation $d \geq 2.75\,\sigma$ (the branches of A and B on opposite sides of a plane, at normal distance $\geq d$), nor at closest approach $d \geq 3.78\,\sigma$.*

The bound on s combines four rigorous inequalities (Appendix B); its final maximisation over the two splittings is a floating-point evaluation of cell bounds on a geometric grid, without interval arithmetic. It gives 0.70456 at $2.75\,\sigma$ (slab) and 0.70457 at $3.78\,\sigma$ (closest approach), 0.36% below $1/\sqrt{2}$, and exceeds $1/\sqrt{2}$ at $2.735\,\sigma$ (0.70875) and $3.765\,\sigma$ (0.71019). A numerical search over all two-branch geometries (differential evolution followed by Nelder–Mead, over several parametrisations) found nothing above $f(d)/f_0$ at slab separation, or above $\max(f(d)/f_0, \text{straddle limit})$ at closest approach; we have not proven these to be the suprema. So at $C = 1$ the largest two-branch distance lies in $[2.2109, 2.75]\,\sigma$ (slab) and $[2.7381, 3.78]\,\sigma$ (closest approach), and equals $2.2109\,\sigma$ within the parallel class.

3.2 Many branches: no critical distance

Theorem 3.3 (No critical distance)**.** *For every $d > 0$ and every $C < \infty$ there are finite branch sets at slab separation d with $\rho_{\max} > s_*$. For uniform coaxial discs of radius a at gap d (lattices of point branches), each body carrying in addition a far copy of its disc,*

$$\rho_{\max} \geq \operatorname{erf}(d/2\sigma)\Big(1 - \frac{3\pi d}{8a}\Big), \tag{12}$$

so the model entangles such states once $a/d > (3\pi/8)/(1 - s_*/\operatorname{erf}(d/2\sigma))$, which is 4.022 at $C = 1$ and $d \gg \sigma$.

The condition is on the extent of the coherent superposition in units of the gap, not on d/σ. The far copy makes the disc pattern neutral without changing the correlation; it means that the coherent extent of the state is really the distance to the copy. The sharp version of this

extent law is in Section 4.3. Since $\rho_{\max} = 1$ for every pair of open supports (Remark 2.3), the absence of a critical distance is not by itself a physical prediction. What matters is how much entanglement the model can produce, and how fast.

4 The entangling rate against the model's own dephasing

4.1 The first-order rate

For equal masses write the rate (8) as $\dot{\lambda} = -\kappa\, Gm^2/(\hbar d)$, with d the separation and $\kappa \geq 0$ dimensionless. Eq. (8) is also the initial rate when a local Hamiltonian is present [9].

Theorem 4.1 (Rate bounds)**.** *Let* $\theta = \min(1, s_*/\rho_{\max})$.

(i) For every product state with closest approach d *and every* σ, $\kappa \leq (1-\theta)\sqrt{1+C^2}\, df(d) \leq \sqrt{1+C^2} - C$, *which is* 0.4142 *at* $C = 1$.

(ii) For supports separated by a slab of width d, *with the Coulomb kernel* ($\sigma \to 0$),

$$\kappa \leq B(C) = \sqrt{1+C^2} - C - C \ln \frac{\sqrt{1+C^2}}{C}, \tag{13}$$

$B(1) = 0.067640$, $B(C) \to 1/(8C^3)$ *for* $C \to \infty$. *For planar supports at finite* σ *the corresponding bound is larger,* 0.104 *at* $d = 3\,\sigma$ *and* $C = 1$, *so* (13) *is a statement for* $\sigma \ll d$.

Explicit states bound the best κ from below. Give each mass an equal superposition of a planar sheet and a far copy of it, the two sheets facing each other at gap d, in the formal limits $\sigma \to 0$ and zero thickness. A Gaussian sheet of rms width b has, for its natural witness,

$$\kappa_G = \max_y \frac{\sqrt{\pi}}{2}\, y\big[\sqrt{1+C^2}\, e^{y^2}\, \mathrm{erfc}(y) - C\big], \qquad y = \frac{d}{2b}, \tag{14}$$

$\kappa_G = 0.027108$ at $b = 3.15\, d$ ($C = 1$); a uniform disc gives 0.0264 at $a = 6.12\, d$. So at $C = 1$ and $\sigma \ll d$ the best rate constant of slab-separated states lies between 0.027 and 0.068. Both explicit values are proven formulas for one witness each, in limits we do not control; at finite d/σ smearing raises them by corrections of first order in σ/d.

4.2 The ratio to the dephasing rate

In the same dynamics the coherence between two branches a, a' of one body decays at the Diósi–Penrose rate $C\, Gm^2[f(0) - f(|a-a'|)]/\hbar$. Because the body is rigid and only its centre is delocalised, this saturates for $|a-a'|$ larger than a few σ_{eff}:

$$\Gamma_{\mathrm{sat}} = \frac{C\, Gm^2 K_0}{\hbar}, \qquad K_0 = \frac{1}{\sqrt{\pi}\,\sigma_{\mathrm{eff}}}, \tag{15}$$

with $\sigma_{\mathrm{eff}} = \sigma$ for point masses and $K_0 = 6/(5R)$, $\sigma_{\mathrm{eff}} = 5R/(6\sqrt{\pi}) = 0.470\, R$, for uniform spheres of radius $R \gg \sigma$. A wide superposition does not dephase faster per pair; every pair of sites further apart than σ_{eff} already dephases at Γ_{sat}. For extended bodies Theorem 2.2 and the bounds hold verbatim with f replaced by the Coulomb energy $K(r)$ of two smeared

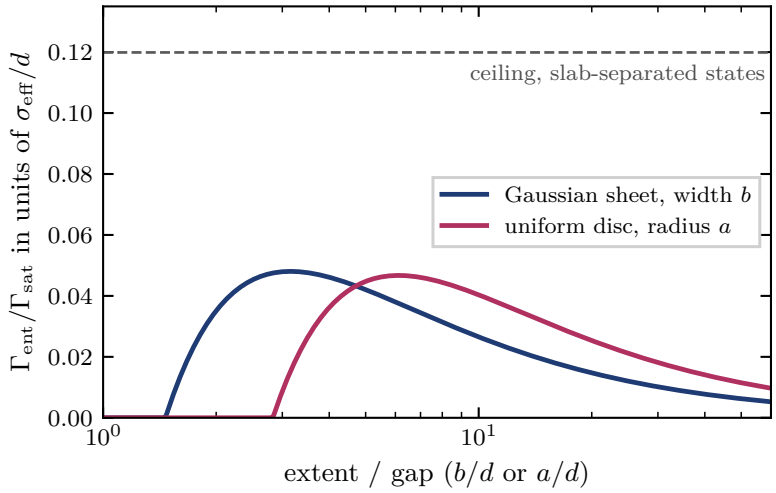


Figure 2. *Entangling rate over single-body dephasing rate, in units of $\sigma_{\rm eff}/d$, at $C = 1$, for a Gaussian sheet of rms width b and a uniform disc of radius a (each with a far copy, $\sigma \to 0$), against the extent in units of the gap. The dashed line is the ceiling (13) for all slab-separated states.*

bodies, which is $1/r$ beyond contact; at large separation only the self-term K_0 changes. With $\Gamma_{\rm ent} = |\dot\lambda| = \kappa\, Gm^2/(\hbar d)$,

$$\mathcal{R} \equiv \frac{\Gamma_{\rm ent}}{\Gamma_{\rm sat}} = \frac{\kappa}{CK_0 d} = \frac{\sqrt{\pi}\,\kappa}{C}\,\frac{\sigma_{\rm eff}}{d}. \tag{16}$$

This is an identity; its bounds are those of Theorem 4.1 (Table 2, Fig. 2). At large C, $\mathcal{R} \le (\sqrt{\pi}/8C^4)\,\sigma_{\rm eff}/d$ for slab-separated supports. At $C = 1$ each body's coherence is lost at least $8.3\,d/\sigma_{\rm eff}$ times faster than entanglement is generated (slab-separated, $\sigma \ll d$), and $20.8\,d/\sigma_{\rm eff}$ times faster for the best state known. As a function of the extent $\mathcal{R}$ vanishes below a threshold ($b/d \le 1.465$ for Gaussian sheets at $C = 1$), peaks near an extent of a few gaps, and falls off like gap over extent beyond: a wider sheet is not better.

Table 2. *The ratio $\mathcal{R} = \Gamma_{\rm ent}/\Gamma_{\rm sat}$ in units of $\sigma_{\rm eff}/d$. The first column is the Gaussian sheet of Eq. (14) ($\sigma \to 0$, zero thickness); the second the slab bound (13) ($\sigma \ll d$); the third Theorem 4.1(i), any product state, any σ.*

C	Gaussian sheets	slab-separated, ceiling	any product state, ceiling
1	0.0481	0.120	0.734
1.25	0.0235	0.0590	0.497
2	0.00453	0.0115	0.209
5	0.000135	0.00034	0.035

The dephasing is already inside the criterion. The first term of the numerator of (8), C times the Coulomb self-energy of the witness pattern, is the Diósi–Penrose dephasing rate of the collective coherence that the witness reads. For a smooth pattern over n point-like branches it consists of a collective part and the point self-energies $f_0 \sum |q(a)|^2$, which are diluted as $1/n$. To leading order, the criterion $\rho_{\max} > s_*$ then reads $n\,\mathcal{R}_{\rm coll} > 1$, with $\mathcal{R}_{\rm coll}$ the ratio of the collective rate to $\Gamma_{\rm sat}$: the saturated dephasing enters divided by the number of branches.

4.3 The extent law

For coaxial discs of radius a at gap $d \gg \sigma$, each with a far copy, the criterion becomes scale-free (formal limit $\sigma \to 0$, zero thickness). The uniform pattern is a witness if and only if

$$\Phi(a/d) > s_*, \qquad \Phi(x) = \frac{3\pi}{16} \int_0^\infty \Big(\frac{2J_1(u)}{u}\Big)^2 e^{-u/x}\, du. \tag{17}$$

For all axisymmetric patterns, writing the Hankel transform of the charge as an Abel transform $\hat{q}(k) = \int_0^1 g(t)\cos(kt)\, dt$ turns the canonical correlation into the top eigenvalue of Love's operator for the circular plate condenser [16],

$$(T_\delta g)(t) = \frac{1}{\pi} \int_{-1}^{1} \frac{\delta\, g(s)}{\delta^2 + (t-s)^2}\, ds, \qquad \delta = d/a, \tag{18}$$

and the criterion is $\lambda_{\max}(T_{d/a}) > s_*$ (Appendix B). Table 3 gives the thresholds; the eigenvalues are computed by Nyström discretisation and are converged. At $C = 1$ the coherent diameter must exceed 5.54 gaps (5.66 for uniform amplitude); at large C, $1 - \Phi \simeq (3\pi/8)\, d/a$ gives $a/d \simeq (3\pi/4)C^2 = 2.356\, C^2$ for the uniform pattern. Without the far copy, the best neutral pattern found on a single disc is dipolar, the odd block of Love's operator: it needs $a/d > 7.390$, a coherent diameter of 14.8 gaps, against 11.34 (22.7 gaps) for the best axisymmetric neutral pattern. In a lattice with spacing larger than σ, reaching the threshold needs at least about $15\, d/\sigma$ point-like branches per mass (numerically, $15.2\, d/\sigma$ at $d = 12\,\sigma$ and $15.6\, d/\sigma$ at $d = 24\,\sigma$, hexagonal patches with a far copy at $C = 1$).

Table 3. *Smallest a/d for which discs of radius a at gap d (each with a far copy, $\sigma \ll d$) are entangled: uniform pattern, Eq. (17); optimal axisymmetric pattern, Eq. (18).*

C	uniform pattern	optimal axisymmetric pattern
1	2.8316	2.7706
1.25	4.1316	4.0642
2	9.7539	9.6453
5	58.810	58.041

4.4 The negativity

Below, the negativity is $|\lambda_{\min}(\rho_t^{T_1})|$, the quantity plotted in [9].

Theorem 4.2 (Negativity bound)**.** *For $H = 0$, equal masses, any product state with weights p, r on finite branch sets, θ as in Theorem 4.1, and all $t' = Gm^2 t/(\hbar\sigma) \geq 0$ (lengths in units of σ),*

$$|\lambda_{\min}(\rho_t^{T_1})| \leq (1-\theta)\, t' \Big\{ \sum p_a p_{a'} r_b r_{b'}\, (C^2\delta^2 + \epsilon^2)\, e^{-2t'C\,(D_A + D_B + \min(\theta\delta, \delta))} \Big\}^{1/2}, \tag{19}$$

the sum over all a, a', b, b', with $\epsilon = F(a,b) - F(a',b')$. If the branches of each mass are at least ℓ apart, $D_\ell = f_0 - f(\ell) > f(d)$ and $C \geq 1/\sqrt{3}$, then $\sup_t |\lambda_{\min}| \leq (1-\theta)(f(d)/e)\big[1/(D_\ell - f(d)) + \sqrt{\sum p^2 + \sum r^2}/(CD_\ell)\big]$; for $\ell, d \gg \sigma$ and many branches this is at most $(\sqrt{\pi}/e)(1 - s_*)\, \sigma/d$: $0.191\, \sigma/d$ at $C = 1$, $0.069\, \sigma/d$ at $C = 2$.

The proof (Appendix B) compares with the model whose cross kernel is θF, which is separable by Remark 2.1. The clean σ/d form needs branches more than a few σ apart; for states with

structure below σ the sum (19) has to be evaluated as it stands, and a σ/d bound for all product states is not proven.

A leading-order law. Expanding the exact matrix elements to first order in the cross kernel, with the local dephasing kept exactly, gives for n branches per mass with uniform weights $n\lambda_{\min} \simeq e^{-2\tau}[e^{\tau} - 1 - \xi\tau]$ up to terms of relative order $1/n$, $\tau = \Gamma_{\rm sat}t$, with $\xi = n\mathcal{R}_{\rm coll}$ the quantity whose exceeding one is the criterion. The factor $e^{-2\tau}$ is the survival of one coherence on each body, $e^{\tau} - 1$ the mixedness the dephasing creates in the witness subspace, $-\xi\tau$ the entangling term. For $\xi \gg 1$,

$$\lambda_{\min}(t) \simeq -\Gamma_{\rm ent}\, t\, e^{-2\Gamma_{\rm sat}t}, \qquad \max_t |\lambda_{\min}| \simeq \frac{\mathcal{R}}{2e} = \frac{\sqrt{\pi}}{2e}\,\frac{\kappa}{C}\,\frac{\sigma_{\rm eff}}{d} \quad \text{at} \quad t_* = \frac{1}{2\Gamma_{\rm sat}}. \tag{20}$$

For Gaussian sheets at $C = 1$ this is $8.8 \times 10^{-3}\,\sigma_{\rm eff}/d$, and the slab ceiling would give $2.2 \times 10^{-2}\,\sigma_{\rm eff}/d$ if the law holds. At finite ξ, n times the peak is $\xi/2e - 0.239 + O(1/\xi)$, and it vanishes at $\xi = 1$. We have derived Eq. (20); we have not bounded its error. Compared with exact partial transposes of uniform lattice sheets at $C = 1$ it agrees to a few per cent; at $C = 2$ it overestimates the exact peak. Because $\mathcal{R}$ multiplies a dephasing time, "negativity of order $10^{-2}\,\sigma/d$" is the statement that the entangling rate is a fraction of the dephasing rate, not an extra suppression.

An explicit state. Take for each mass a hexagonal patch of 19 point branches with spacing $8\,\sigma$, plus its far copy (38 branches per mass), the two patches facing each other at slab separation $d = 3.52\,\sigma$, beyond the two-branch ceiling of Proposition 3.2, and $C = 1$. Then $\rho_{\max} = 0.813 > s_*$, $\kappa = 0.0258$, $\mathcal{R} = 0.0130$ and $\mathcal{R}/2e = 2.4 \times 10^{-3}$. Exact diagonalisation of the 1444-dimensional partial transpose gives a smallest eigenvalue of -1.6×10^{-3} at $t' = 0.5$, when each body's coherence is still 0.75; the peak lies below the large-ξ value because this state is sparse. Unitary Newtonian gravity ($1/r$ coupling, no noise) on the same state reaches -0.41.

For extended bodies Eq. (20) holds with $\sigma_{\rm eff}$; for spheres with $\sigma \ll R$ the negativity of sheet states is floored by the radius, $\sigma_{\rm eff} = 0.470\,R$, however small σ is.

5 The Bose *et al.* design and the inference from an observation

5.1 Numbers

In the design of [1] the branches of A sit at 0 and 250 μm, those of B at 450 and 700 μm, collinear, with closest approach $d = 200$ μm and $m = 10^{-14}$ kg (a diamond sphere of radius $R = 0.879$ μm). The configuration is parallel (Theorem 3.1), and Eq. (10) shows that the model entangles it if and only if $\sigma > 524.494$ μm at $C = 1$ (617, 910 and 2158 μm at $C = 1.25$, 2, 5). At $\sigma = 524$ μm the smeared force between two point masses 1 mm apart is 0.39 of its Newtonian value; torsion-balance tests of the inverse-square law at such separations show no deviation at that level [17]. No two-branch geometry with closest approach 200 μm is entangled unless $\sigma > 73.0$ μm (straddle) or 90.5 μm (slab), according to the numerical suprema of Section 3, and Proposition 3.2 guarantees $\sigma > 52.9$ μm (any geometry) or 72.7 μm (slab).

Many-branch states at the same separation are entangled for any σ, but at the rates of Section 4. For $\sigma \ll R$ and $C = 1$ each body dephases at $\Gamma_{\rm sat} = 86$ s^{-1} (coherence time 11.6 ms; over the 2.5 s of the proposed experiment the dephasing exponent is 216). A Gaussian sheet state of width $b \approx 630$ μm at $d = 200$ μm entangles at $\Gamma_{\rm ent} = \kappa_G G m^2/(\hbar d) = 8.6 \times 10^{-3}$ s^{-1}, so

$\mathcal{R} = 9.9 \times 10^{-5}$, and the law (20) puts the peak negativity at 1.8×10^{-5}, 5.8 ms after preparation. Unitary Newtonian gravity gives the two-branch design an entangling phase of 0.314 rad after 2.5 s.

5.2 What an observed entanglement excludes

Remains true. For two-branch states with ideal branches the model produces no entanglement at any time unless σ is comparable to the separation: below $2.2109\,\sigma$ for parallel superpositions (proven), below $2.75\,\sigma$ at slab separation for any geometry (computer-assisted). In any geometry with branches more than a few σ apart the negativity stays below $0.191\,\sigma_{\text{eff}}/d$ at $C = 1$ (Theorem 4.2), against about 0.4 for unitary gravity. An entanglement signal of the size the quantum prediction gives, or one that oscillates or persists beyond a few dephasing times $1/\Gamma_{\text{sat}}$, is incompatible with the model. Before entanglement is at issue, the survival of each body's superposition over the experiment already tests the model.

No longer true. "The Diósi–Penrose dynamics cannot entangle masses further apart than $0.85\,\sigma$ (or $2.21\,\sigma$)", read as a statement about the model rather than about a two-branch geometry; equivalently, "the dynamics is separability-preserving for $d \gg \sigma$". And the geometry-free inference "any entanglement detected beyond $2.2\,\sigma$ falsifies the model, whatever the state and whatever its size". The inference has to go through the size and the time course of the signal, or be restricted to two-branch geometries. For the design above, with ideal branches, a positive result of the expected size excludes the model for every σ below 524 μm. For wavepackets of finite width the criterion is degenerate (Remark 2.3) and we give no bound on what they produce, so the statement is not extended to any positive result.

Answer to the question of [9]: entanglement from this model can in principle be produced at any separation, with superpositions over many branches whose coherent extent is several times the separation; it is then produced at a rate of order σ/d times the rate at which the superposition itself is destroyed, and, for branches more than a few σ apart, it never exceeds a fraction of order σ/d of what unitary gravity gives.

6 Scope and discussion

Position-eigenstate branches. Theorem 2.2 is exact for branches that are position eigenstates. For square-integrable wavefunctions $\rho_{\max} = 1$ (Remark 2.3): every pair of real wavepackets is entangled at once, and the yes/no question has no content there. For wavefunctions Theorem A.1 gives the entangling direction, with the rate (8) in integral form; the negativity bound (19) is proven for finite branch sets only, and we give no bound in terms of the packet width.

The kinetic term. All results are for $H = 0$. The initial rate (8) and the bounds of Theorem 4.1 are unchanged by any local Hamiltonian defined on the initial state, and local Hamiltonians acting within a finite set of sites cannot make a sub-threshold region entangling (Theorem 2.2(b)). Beyond that we control nothing: free packets acquire full support at once and the negativity bound has not been extended to them. For $m = 10^{-14}$ kg the relevant experiments sit deep in the static regime, which is an argument, not a bound.

Preparation. Every result assumes the product state exists at $t = 0$. The same dephasing acts while it is made: a superposition over at least about $15\,d/\sigma$ positions, more than five gaps across, must be prepared in a time short compared with $1/\Gamma_{\text{sat}}$ (11.6 ms for the mass above), or

it never exists.

What is numerical. The critical distances, the constants Λ_+, $L_{1/2}$, the extent thresholds and the rate constants are roots and maxima of explicit one-dimensional functions, or top eigenvalues of converged discretisations of Love's operator. Proposition 3.2 is computer-assisted, in floating point, without interval arithmetic, with a margin of 0.36%. That the two-branch suprema over all geometries equal the closed forms of Table 1 rests on numerical search. The optimality of the axisymmetric sector on discs, and the identification of the best single-disc pattern as dipolar, are numerical. The leading-order law (20) is derived without an error bound and was compared with exact partial transposes of lattice sheets only; the explicit state of Section 4.4 is one exact instance. Exact partial transposes at larger separations and with more branches agree with the law at $C = 1$; we do not quote them.

Also open. Separability after the negative eigenvalue has returned to zero; the best rate constant, bracketed between 0.027 and 0.068 at $C = 1$; non-planar supports; noise kernels other than the Newtonian one; $C < 1$, which is not a classical model; the variant with an unsmeared force, which is not a measurement-and-feedback model and to which the pair decomposition does not apply.

Discussion. The Diósi–Penrose model is a classical channel with a definite structure: one kernel in force and noise, and a local dephasing equal to the Gram form of that kernel. That structure gives an exact criterion, a canonical correlation against $C/\sqrt{1+C^2}$, and it ties the entangling rate to the model's own dephasing rate by a factor of order σ/d. The model's generator is not separability-preserving at any distance, so it is not a local-operations-and-classical-communication channel. But what it produces at separations large compared with σ is small and short-lived, and it is preceded by the loss of each body's coherence at the Diósi–Penrose rate. For entanglement-witness experiments the useful discriminants are the size and the time course of the signal, and, before them, the survival of the single-body superposition.

A Proof of the separable half, and wavefunctions

Theorem 2.2(b). Absorb the masses into g. Choose orthonormal bases e_i of V_A and e'_i of V_B with $\langle e_i, e'_j\rangle = s_i\delta_{ij}$ (singular value decomposition; $s_1 = \rho_{\max}$, $s_i = 0$ beyond the smaller rank). Fix reference branches a_0, b_0 and put $x_i(a) = \langle e_i, g_a - g_{a_0}\rangle$, $y_i(b) = \langle e'_i, g_b - g_{b_0}\rangle$. Since the $g_a - g_{a'}$ lie in V_A,

$$D_A = \tfrac{1}{2}\sum_i \big(x_i(a) - x_i(a')\big)^2, \qquad \delta = \sum_i s_i\big(x_i(a) - x_i(a')\big)\big(y_i(b) - y_i(b')\big), \tag{21}$$

and $F(a,b) = \sum_i s_i x_i(a) y_i(b) + \varphi_A(a) + \varphi_B(b) + \text{const}$. Hence $\Lambda = \sum_i \Lambda_i + i[\varphi_A(a) - \varphi_A(a')] + i[\varphi_B(b) - \varphi_B(b')]$ with Λ_i as in Eq. (9); the phases φ are local unitaries. For each i take real Gaussian variables $(\eta_i, \zeta_i, \eta'_i, \zeta'_i)$, mean zero, independent for different i, with covariance

$$t\, s_i \begin{pmatrix} |J| & J \\ J & |J| \end{pmatrix}, \qquad J = \begin{pmatrix} 0 & \frac{1}{2} \\ \frac{1}{2} & C \end{pmatrix}, \tag{22}$$

positive semidefinite because $|J| \pm J \geq 0$. Define the random diagonal operators $U_A = \sum_a \exp[\sum_i x_i(a)(\eta_i + i\zeta_i)]\,|a\rangle\langle a|$ and U_B likewise with y_i, η'_i, ζ'_i. With $\mathbb{E}\, e^Z = e^{\mathbb{E}[Z^2]/2}$ the

cross covariances $\mathbb{E}[\zeta_i\zeta_i'] = ts_iC$ and $\mathbb{E}[\eta_i\zeta_i'] = \mathbb{E}[\zeta_i\eta_i'] = ts_i/2$ give

$$\mathbb{E}\big[u_A(a)u_B(b)\bar{u}_A(a')\bar{u}_B(b')\big] = \exp\Big\{t\sum_i s_i\big[i(x_iy_i - x_i'y_i') - C(x_i - x_i')(y_i - y_i')\big]\Big\}\, L_A(a,a')L_B(b,b'), \tag{23}$$

using $(x+x')(y-y') + (x-x')(y+y') = 2(xy - x'y')$, with local factors L. Dividing, $e^{t\Lambda} = \mathbb{E}[u\bar{u}]\, T_A(a,a')T_B(b,b')$ up to the local phases, with

$$T_A(a,a') = d(a)\overline{d(a')}\,\exp\Big\{t\sum_i (C - s_i\,\mathrm{tr}\,|J|)x_i(a)x_i(a')\Big\}, \qquad \mathrm{tr}\,|J| = \sqrt{1+C^2}, \tag{24}$$

d a non-vanishing diagonal factor, and the same for T_B. If $s_i\sqrt{1+C^2} \le C$ for all i the exponent is t times a positive semidefinite matrix; its entrywise exponential is positive semidefinite by the Schur product theorem [15], so T_A and T_B act as completely positive Schur multipliers $\mathcal{T}_A$, $\mathcal{T}_B$. Therefore

$$\rho_t = \mathbb{E}\Big[(U_A \otimes U_B)\,(\mathcal{T}_A \otimes \mathcal{T}_B)(\rho_0)\,(U_A \otimes U_B)^\dagger\Big], \tag{25}$$

a mixture of products of local completely positive maps, trace preserving in total because the diagonal of $e^{t\Lambda}$ is one. Separable states go to separable states. Interleaved local channels and the Lie–Trotter limit in finite dimension, with the separable set closed, give the last statement. The construction needs only that the Gram matrices f_A, f_B are non-singular (distinct branches); it holds for any number of branches, any amplitudes and every $t \ge 0$. If $\rho_{\max} > s_*$, then T_A and T_B are indefinite and part (a) shows the state entangled. □

Theorem A.1 (Wavefunctions, entangling direction)**.** *Let $\psi_A, \psi_B \in L^2(\mathbb{R}^3)$ and $H = 0$. Suppose there are bounded neutral q_1, q_2, supported on sets of finite measure on which $|\psi_A|, |\psi_B| \ge \varepsilon > 0$, with $C\langle q_1,q_1\rangle + C\langle q_2,q_2\rangle - 2\,\mathrm{Re}[(C+i)\langle q_1,q_2\rangle] < 0$ in the smeared Coulomb form. Then ρ_t is entangled for all sufficiently small $t > 0$.*

Proof. The kernel Λ is bounded ($|f| \le f_0$). With $c = q_1 \otimes |\psi_B|^2 + |\psi_A|^2 \otimes q_2 \in L^1$ and $\chi = c/\tilde{\Psi}^* \in L^2$, $\langle\chi|\rho_t^{T_1}|\chi\rangle = \iint \bar{c}\,c\,e^{t\Lambda} = t\,(\text{negative}) + O(t^2\|c\|_1^2)$. A separable state has a positive partial transpose, whose quadratic form is non-negative. □

Since the smeared point charges of any open set span the Coulomb space (their potentials are real-analytic), such q_1, q_2 exist for every pair of supports with interior and every separation.

B Proofs of the bounds

Lengths are in units of σ unless stated.

Theorem 3.1. $h(x) = f(\sqrt{x}) = \pi^{-1/2}\int_0^1 e^{-xu^2/4}du$ is a mixture of decaying exponentials: decreasing, convex and log-convex. Put $x = |r|^2$, $y = |w|^2$, $P = |r-w|^2$, $Q = |r+w|^2$, so $P + Q = 2x + 2y$, and $N = 2h(x) - h(P) - h(Q)$, $s = |N|/(2D(|w|))$. If $N > 0$: convexity gives $h(P) + h(Q) \ge 2h(x+y)$, log-convexity $h(x+y)h(0) \ge h(x)h(y)$, so $N \le 2[h(x) - h(x+y)] \le 2(f(|r|)/f_0)\,D(|w|)$, and $|r| \ge d$. If $N < 0$: (i) $-N$ is the second difference of $t \mapsto f(|r+tw|)$ at $t = -1, 0, 1$, hence $\le |w|^2\Lambda_+$, with Λ_+ the largest Hessian eigenvalue of f over space, which is $\max f''$ because $f' < 0$; (ii) with $P \le Q$ the parallelogram law gives $Q \ge x$, so $-N \le h(P) - h(x) \le f(d)$. For $|w| \ge L_{1/2}$, (ii) gives $-N/(2D) \le f(d)/f_0$. For $|w| \le L_{1/2}$, (i)

gives $-N/(2D) \le \Lambda_+|w|^2/(2D(|w|)) \le \Lambda_+ L_{1/2}^2/f_0$, because $L^2/D(L)$ is increasing ($D(L)/L^2$ is a difference quotient of the convex h). The transversal family with $L \to \infty$ approaches $f(d)/f_0$ from below. □

Proposition 3.2. Write $N = \psi(b_1) - \psi(b_2)$ with $\psi(b) = f(|b-a_1|) - f(|b-a_2|)$. (i) $|\psi| \le g_d L_A$ with $g_d = \sup_{r \ge d} |f'|$. (ii) $|\psi| \le m_d(L_A)$, $m_d(L) = \sup_{r \ge d}[f(r) - f(r+L)]$. The same with A and B exchanged. (iii) N is a double difference, so $|N| \le L_A L_B \sup \|\nabla^2 f\|$ over the parallelogram of difference vectors, on which $|x| \ge d$ at slab separation and $|x| \ge d - (L_A + L_B)/2$ at closest approach; $\|\nabla^2 f\| = \max(|f''|, |f'|/r) \le \kappa_0$. Then

$$s \le \frac{\min\{2g_d L_A,\, 2g_d L_B,\, 2m_d(L_A),\, 2m_d(L_B),\, H L_A L_B\}}{2\sqrt{D(L_A) D(L_B)}}, \tag{26}$$

with H the supremum in (iii), maximised over (L_A, L_B) with cell bounds (numerators at the upper corner, denominators at the lower corner of each cell of a geometric grid of ratio 1.01, a last cell for $L > 400\,\sigma$), using that $L/\sqrt{D(L)}$, m_d and D are monotone. The suprema over r are taken on grids. The bound is non-increasing in d and crosses $1/\sqrt{2}$ where stated in Section 3. □

Theorem 3.3. Smearing lowers the self-energy, so $\langle q, q\rangle \le 16/(3\pi a)$ per unit-charge uniform disc; $f(r) \ge \operatorname{erf}(d/2\sigma)/r$ for $r \ge d$; and for unsmeared coaxial discs $E(0) - E(d) = \int \frac{d^2k}{(2\pi)^2} \frac{2\pi}{k} |\hat{q}|^2 (1 - e^{-kd}) \le 2\pi d \int q^2 = 2d/a^2$. The far copy makes the pattern neutral without changing the ratio; this proves (12). For the first statement at arbitrary d and C, let A carry a uniform planar lattice patch (with in-plane distances $\Delta_{jj'}$) and its far copy, and B the same patch translated by d along the normal. The same Fourier estimate, with the smeared kernel, gives $1 - \rho_{\max} \le (d/2\sigma^2) \sum_{jj'} e^{-\Delta_{jj'}^2/4\sigma^2} / \sum_{jj'} f(\Delta_{jj'})$; the numerator grows like the number of points and the denominator like its square times f of the patch size, so the right side tends to zero for growing patches. As wavefunctions, discs of small thickness inherit a strict inequality by continuity of the bounded smeared kernel. □

Extent law. For charges on coaxial unit discs at gap δ ($\sigma \to 0$), the mutual energy is, up to a common constant, $E(\delta) = \int_0^\infty e^{-k\delta} \hat{q}(k)^2 dk$, with $\hat{q}$ the Hankel transform of the charge. Writing an axisymmetric charge through its Abel transform, $\hat{q}(k) = \int_0^1 g(t) \cos(kt)\, dt$ with g extended evenly to $(-1, 1)$, gives $E(0) = (\pi/2) \int_0^1 g^2$ and $E(\delta) = (\pi/2) \int_0^1 g\, T_\delta g$, with T_δ of Eq. (18), the operator of Love's integral equation [16]. The canonical correlation is the top eigenvalue of T_δ on even functions. The uniform disc is $g(t) = \sqrt{1 - t^2}$, for which the Rayleigh quotient is Φ of Eq. (17). □

Theorem 4.1. (i) $C\langle q_1, q_1\rangle + C\langle q_2, q_2\rangle \ge 2C|\langle q_1, q_2\rangle|/\rho_{\max}$, so the numerator of (8) is $\ge -2(1-\theta)\sqrt{1 + C^2}|\langle q_1, q_2\rangle|$, and $|\langle q_1, q_2\rangle| \le f(d)\|q_1\|_1 \|q_2\|_1 \le \frac{1}{2} f(d)(\sum |q_1|^2/p + \sum |q_2|^2/r)$ by Cauchy–Schwarz. (ii) For charges at depths $z \le 0$ and $z' \ge d$, $\langle q_1, q_2\rangle = \int \frac{d^2k}{(2\pi)^2} \frac{2\pi}{k} e^{-kd} \bar{A}_1 A_2$ with $A_1(k) = \int dz\, e^{kz} \hat{q}_1(k, z)$, $|A_1| \le \|q_1\|_1$, and $\langle q_1, q_1\rangle \ge \int \frac{d^2k}{(2\pi)^2} \frac{2\pi}{k} |A_1|^2$, because $e^{-k|z-z'|} - e^{k(z+z')}$ is $2k$ times the Dirichlet Green function of $-\partial_z^2 + k^2$ on the half-line, a positive kernel. Then mode by mode the numerator is at least $-\int \frac{d^2k}{(2\pi)^2} \frac{2\pi}{k} [\sqrt{1 + C^2} e^{-kd} - C]_+ (|A_1|^2 + |A_2|^2)$, and $\int_0^\infty [\sqrt{1 + C^2} e^{-kd} - C]_+ dk = B(C)/d$. With smearing, for planar supports, e^{-kz} is replaced by $w(k, z) = \frac{1}{2}[e^{-kz} \operatorname{erfc}(\sigma k - z/2\sigma) + e^{kz} \operatorname{erfc}(\sigma k + z/2\sigma)]$, which gives the finite-σ value quoted.

Eq. (14) is the rate of the witness proportional to the sheet profile, evaluated with the same mode formula. □

Theorem 4.2. Let Λ_θ be Λ with F replaced by θF in the Hamiltonian and in the correlated noise, local dephasing unchanged, and $\rho_t^\theta = \rho_0 \circ e^{t'\Lambda_\theta}$. Its canonical correlations are $\theta s_i \le s_*$, so by Remark 2.1 ρ_t^θ is separable and $(\rho_t^\theta)^{T_1} \ge 0$. Now $\rho_t = \rho_t^\theta \circ M$ with $M = \exp[t'(1-\theta)(i\epsilon - C\delta)]$, so by Weyl's inequality $\lambda_{\min}(\rho_t^{T_1}) \ge -\|\rho_t^\theta \circ (M-1)\|_{\mathrm{HS}}$, the Hilbert–Schmidt norm being invariant under partial transposition. Entrywise $|\rho_t^\theta| = (p_a p_{a'} r_b r_{b'})^{1/2} e^{-t'C(D_A+D_B+\theta\delta)}$ and $|M-1| \le t'(1-\theta)(\epsilon^2 + C^2\delta^2)^{1/2} \max(1, e^{-t'(1-\theta)C\delta})$; every exponent is non-positive since $D_A + D_B + \delta = \frac{1}{2}\|g_a - g_{a'} + g_b - g_{b'}\|^2 \ge 0$. For the corollary: terms with $a \ne a'$, $b \ne b'$ have $C^2\delta^2 + \epsilon^2 \le 4C^2 f(d)^2$ (for $C \ge 1/\sqrt{3}$) and exponent $\ge 2D_\ell - 2f(d)$; terms with one index pair equal have $\delta = 0$, $|\epsilon| \le f(d)$, exponent $\ge D_\ell$ and weight $\sum p^2$ or $\sum r^2$; and $\sup_t te^{-\alpha t} = 1/(e\alpha)$. For $\ell, d \gg \sigma$, $D_\ell \to f_0 = 1/\sqrt{\pi}$ and $\sum p^2, \sum r^2 \to 0$. □

References

[1] S. Bose, A. Mazumdar, G. W. Morley, H. Ulbricht, M. Toroš, M. Paternostro, A. A. Geraci, P. F. Barker, M. S. Kim, and G. Milburn, *Spin Entanglement Witness for Quantum Gravity*, Phys. Rev. Lett. **119**, 240401 (2017). doi:10.1103/PhysRevLett.119.240401

[2] C. Marletto and V. Vedral, *Gravitationally Induced Entanglement between Two Massive Particles is Sufficient Evidence of Quantum Effects in Gravity*, Phys. Rev. Lett. **119**, 240402 (2017). doi:10.1103/PhysRevLett.119.240402

[3] L. Diósi, *A universal master equation for the gravitational violation of quantum mechanics*, Phys. Lett. A **120**, 377 (1987). doi:10.1016/0375-9601(87)90681-5

[4] L. Diósi, *Models for universal reduction of macroscopic quantum fluctuations*, Phys. Rev. A **40**, 1165 (1989). doi:10.1103/PhysRevA.40.1165

[5] R. Penrose, *On gravity's role in quantum state reduction*, Gen. Relat. Gravit. **28**, 581 (1996). doi:10.1007/BF02105068

[6] A. Tilloy and L. Diósi, *Sourcing semiclassical gravity from spontaneously localized quantum matter*, Phys. Rev. D **93**, 024026 (2016). doi:10.1103/PhysRevD.93.024026

[7] A. Tilloy and L. Diósi, *Principle of least decoherence for Newtonian semiclassical gravity*, Phys. Rev. D **96**, 104045 (2017). doi:10.1103/PhysRevD.96.104045

[8] D. Kafri, J. M. Taylor, and G. J. Milburn, *A classical channel model for gravitational decoherence*, New J. Phys. **16**, 065020 (2014). doi:10.1088/1367-2630/16/6/065020

[9] D. Trillo and M. Navascués, *The Diósi–Penrose model of classical gravity predicts gravitationally induced entanglement*, Phys. Rev. D **111**, L121101 (2025). doi:10.1103/PhysRevD.111.L121101

[10] O. Angeli and M. Carlesso, *Entanglement in Markovian hybrid classical-quantum theories of gravity*, Phys. Rev. D **112**, 024047 (2025). doi:10.1103/jzht-fbwt

[11] A. Di Biagio, *Gravity-induced entanglement is not a theory-independent witness of nonclassicality of the gravitational field*, arXiv:2511.02683 (2025). arXiv:2511.02683

[12] Y.-X. Wang, J. S. Pedernales, and M. B. Plenio, *Recoverability of Gravitational Entanglement under Decoherence*, arXiv:2611.05044 (2026). arXiv:2611.05044

[13] H. Hotelling, *Relations Between Two Sets of Variates*, Biometrika **28**, 321 (1936). doi:10.1093/biomet/28.3-4.321

[14] A. Peres, *Separability Criterion for Density Matrices*, Phys. Rev. Lett. **77**, 1413 (1996). doi:10.1103/PhysRevLett.77.1413

[15] R. A. Horn and C. R. Johnson, *Matrix Analysis*, 2nd ed. (Cambridge University Press, 2013). ISBN 9780521839402.

[16] E. R. Love, *The Electrostatic Field of Two Equal Circular Co-axial Conducting Disks*, Q. J. Mech. Appl. Math. **2**, 428 (1949). doi:10.1093/qjmam/2.4.428

[17] J. G. Lee, E. G. Adelberger, T. S. Cook, S. M. Fleischer, and B. R. Heckel, *New Test of the Gravitational $1/r^2$ Law at Separations down to 52 μm*, Phys. Rev. Lett. **124**, 101101 (2020). doi:10.1103/PhysRevLett.124.101101